Preparation of 3-Bromo-1,2,4,5-tetrazine

Hoff, Lukas V ; Schnell, Simon D ; Benchimol, Elie ; Foutinho, Fabio Pereira ; Tomio, Andrea ; Rickhaus, Michel ; Gademann, Karl

DOI: https://doi.org/10.1002/hlca.202200198

doi.org/10.1002/hlca.202200198 SYNTHETIC PROCEDURE HELVETICA chimica acta

Preparation of 3-Bromo-1,2,4,5-tetrazine

Lukas V. Hoff,[a] Simon D. Schnell,[a] Elie Benchimol,[a] Fabio Pereira Foutinho,[a] Andrea Tomio,[a] Michel Rickhaus,[a] and Karl Gademann*[a]

[a] Department of Chemistry, University of Zurich, Winterthurerstrasse 190, CH-8057 Zurich, Switzerland, e-mail: karl.gademann@uzh.ch

In memory of Prof. Dr. *Jack Dunitz*

In this synthetic procedure, a seven-step protocol for the preparation of monosubstituted 3-bromo-1,2,4,5-tetrazine is presented. The procedure features efficient transformations and purification methods starting from commercially readily available starting materials and affords the title compound on a gram scale with 13% overall yield in reliable purity (>97%). Detailed experimental procedures, supported by images and additional notes, allow the preparation of a valuable advanced building block, enabling further applications in bioconjugation, protein labelling, bio-orthogonal chemistry, heterocycle syntheses, high energy materials, and drug release, among others.

Keywords: bioconjugation, bio-orthogonal chemistry, *Diels–Alder* reaction, nitrogen heterocycles, organic materials, synthetic methods, tetrazines.

Introduction

s-Tetrazines are nitrogen-rich heterocycles, which were first described by *Pinner* at the end of the 19th century.[1] Over the years, *s*-tetrazines have become a valuable structural motif in a broad range of chemical fields, including total synthesis, organic electronics, energetic materials and coordination chemistry.[2–6] However, most prominently *s*-tetrazines have become one of the most appreciated functional handles in the field of bio-orthogonal chemistry due to their unparalleled kinetics in inverse electron demand *Diels–Alder* cycloadditions. In this context, the minimal 3-bromo-1,2,4,5-tetrazine was developed. So far, two synthetic procedures to access this 3-bromotetrazine have been published in the literature.[7,8] The first one was published by our group[7] and represents an unoptimized version of the procedures described herein. Besides us, *Riera* and co-workers developed the same reagent and verified its utility for protein labelling and as a possible trigger for click-to-release reactions underlining the high potential of this compound.[8] Their procedure, however, commences with thiocarbohydrazide, a chemical which easily releases toxic hydrogen sulfide gas. Also, the use of elemental bromine renders this approach less attractive. Additionally, the low yield of 22% reported for one step during this synthesis of the title compound leaves room for improvement.

The route described below (*Scheme 1*) from guanidine hydrochloride to **3** and **6** is based on previous reports by *Schirrmacher*[9] and *Hiskey*,[10] respectively, which were extended and optimized. The approach features seven steps with an overall yield of 13% utilizing cheap and commercially available starting materials and reagents as well as efficient purification methods affording all intermediates and the title compound with reliable yield and purity.

Synthetic Procedure (*Notes 1, 2*)

A. 1,2,3-Triaminoguanidine Hydrochloride (1)

A sulfonation flask (1.5 L, four-necked) was equipped with a mechanical overhead stirrer fitted with a water-cooled stirrer bearing, a reflux condenser, a thermometer, and a wide necked glass funnel (NS29) under air

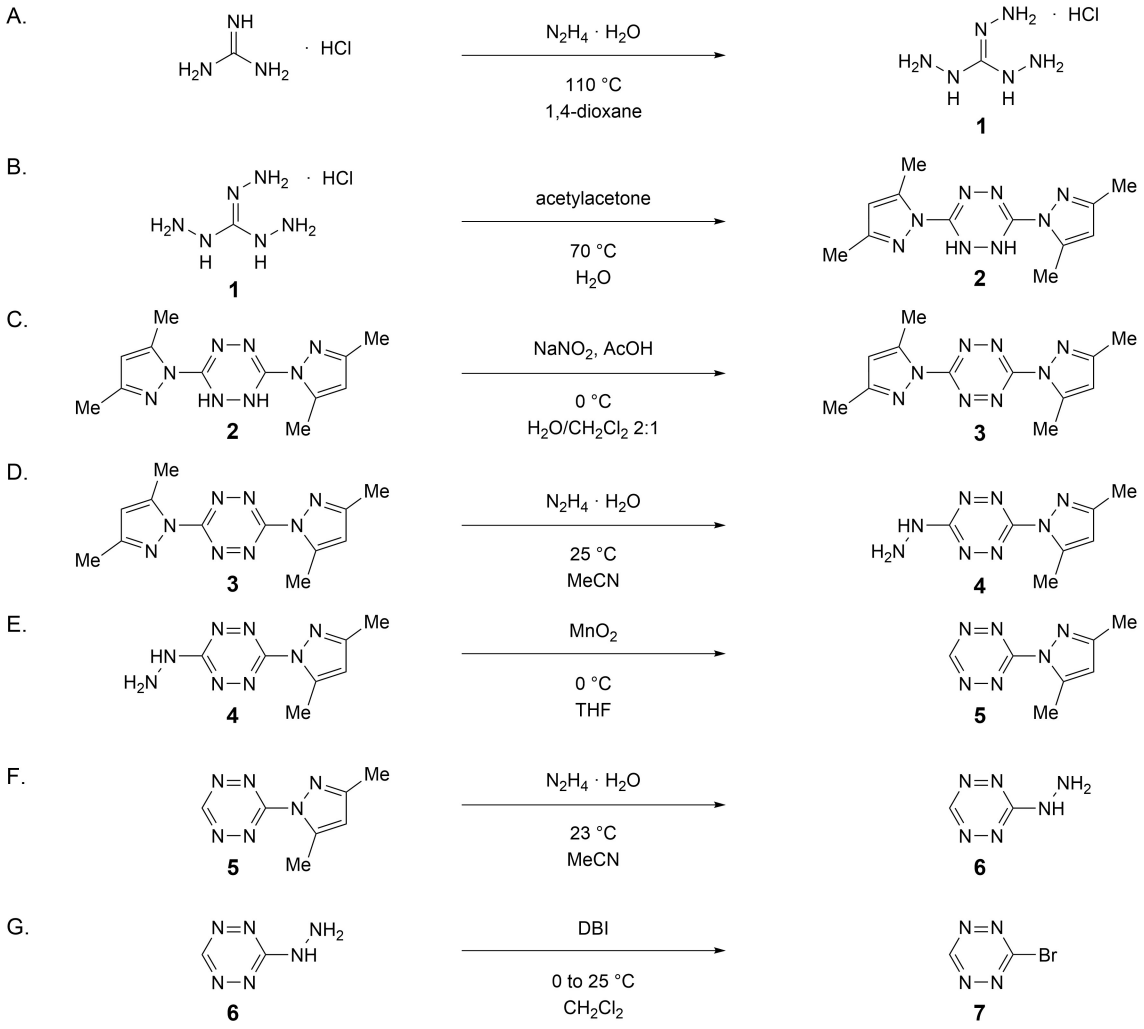

Scheme 1. Overview of the synthesis of monosubstituted bromotetrazine **7**.

atmosphere. Guanidine hydrochloride (40.0 g, 419 mmol, 1.00 equiv.) and 1,4-dioxane (210 mL) were added subsequently by means of the funnel. The stirrer speed was adjusted to ~300 rpm and hydrazine monohydrate (120 mL, 2095 mmol, 5.0 equiv., 17.5M; *Note 3*) was added through the same funnel resulting in complete dissolution of the guanidine hydrochloride and formation of a clear biphasic solution. After complete addition, the funnel was replaced with a glass stopper and the mixture was heated to reflux at 110 °C (bath temperature) by means of an oil bath for 2 h (*Figure 1–1*). During this time, a colorless crystalline solid precipitated. After 2 h, the oil bath was removed, and the mixture was allowed to cool to room temperature (*Note 4*). During cooling to room temperature, a color change of the liquid phase to pale pink/red was observed. The suspension was filtered through a glass filter frit (pore size 4) and the filter cake was rinsed with 1,4-dioxane (3×100 mL) resulting in a yellowish solid (*Figure 1–2*). A second colorless batch was obtained by refiltration of the filtrate. The two batches were combined and dried under high vacuum affording compound **1** (46.0 g, 327 mmol, 78% (71%–82%)) as a colorless crystalline solid (*Figure 1–5*; *Notes 5*, *6* and *7*).

B. 3,6-Bis(3,5-Dimethyl-1*H*-pyrazol-1-yl)-1,2-dihydro-1,2,4,5-tetrazine (**2**)

A sulfonation flask (1.5 L, four-necked) was equipped with a mechanical overhead stirrer fitted with a water-cooled stirrer bearing, a reflux condenser, a thermometer, and a wide necked glass funnel (NS29) under air atmosphere (*Figure 2–1*). The flask was charged with **1**

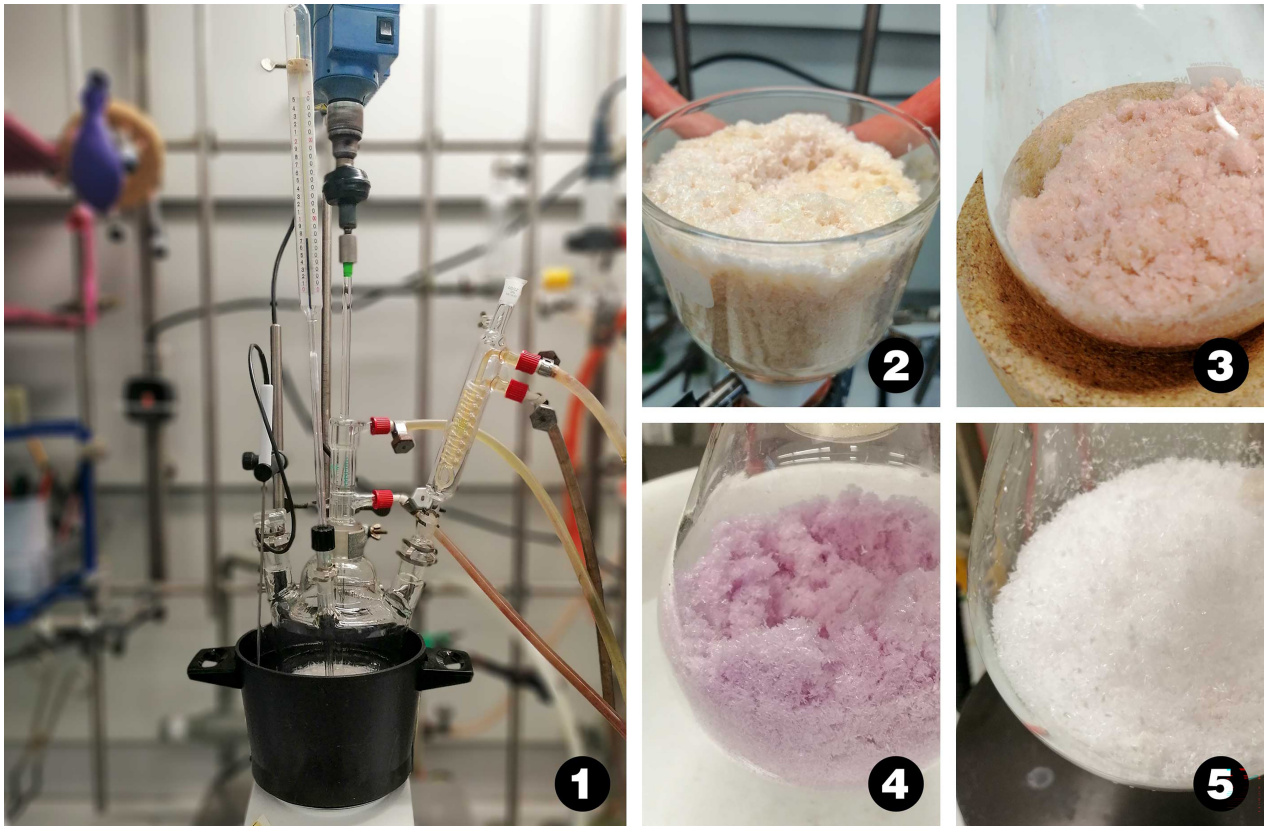

Figure 1. Reaction set-up and color changes of the product **1** during drying. (1) Reaction apparatus. (2) After filtration. (3) After transfer into round bottom flask. (4) After 60 min of drying at high vacuum. (5) After 20 h of drying at high vacuum.

(46.1 g, 328 mmol, 1.00 equiv.) and deionized H_2O (650 mL) by means of the funnel and the stirrer speed was adjusted to ~400 rpm. The funnel was replaced with a dropping funnel (100 mL), which was then charged with acetylacetone (67.0 mL, 656 mmol, 2.00 equiv.). The solution was cooled to below 10 °C internal temperature with an ice/water bath. Acetylacetone was then added dropwise over 20 min, carefully monitoring that the internal temperature did not rise over 15 °C (exothermic reaction!). After complete addition, the funnel was replaced by a glass stopper and the pale yellowish mixture was heated to 70 °C (bath temperature) by means of an oil bath and stirred at this temperature for 16 h (*Note 8*). Within the first 2 h, large amounts of a yellow solid precipitated and the stirrer speed was adjusted to a rate where proper mixing of the suspension was ensured (500–700 rpm; *Figure 2–2*). After 16 h, the yellow suspension was allowed to cool to 25–35 °C (internal temperature) and was filtered through a glass filter frit (pore size 4). The filter cake was washed with cold water (3×230 mL, 4 °C; *Figure 2–3*, *Note 9*). The residue was dried under high vacuum to afford dihydrotetrazine **2** (34.4 g, 126 mmol, 77% (73%–80%)) as a yellow solid (*Figure 2–4*; *Notes 10*, *11*, and *12*).

C. **3,6-Bis(3,5-dimethyl-1*H*-pyrazol-1-yl)-1,2,4,5-tetrazine** (**3**; *Note 13*)

A sulfonation flask (1.5 L, four-necked) was equipped with a mechanical overhead stirrer fitted with an uncooled stirrer bearing, a pressure equalized dropping funnel (250 mL), a thermometer, and a wide necked glass funnel (NS29) under air atmosphere. Dihydrotetrazine **2** (34.4 g, 126 mmol, 1.00 equiv.) and CH_2Cl_2 (150 mL) were added subsequently through the funnel and the suspension was cooled to below 5 °C (internal temperature) by an ice/water bath while stirring (~350 rpm). The funnel was replaced with a glass stopper (*Figure 3–1*). Dropwise addition of a solution of $NaNO_2$ (26.4 g, 378 mmol, 3.00 equiv.) in H_2O (300 mL) through the dropping funnel over 20 min, while maintaining an internal temperature of below 10 °C, resulted in an orange to red biphasic suspension. Subsequently, glacial acetic acid (19 mL, 315 mmol, 2.50 equiv.) was added dropwise through

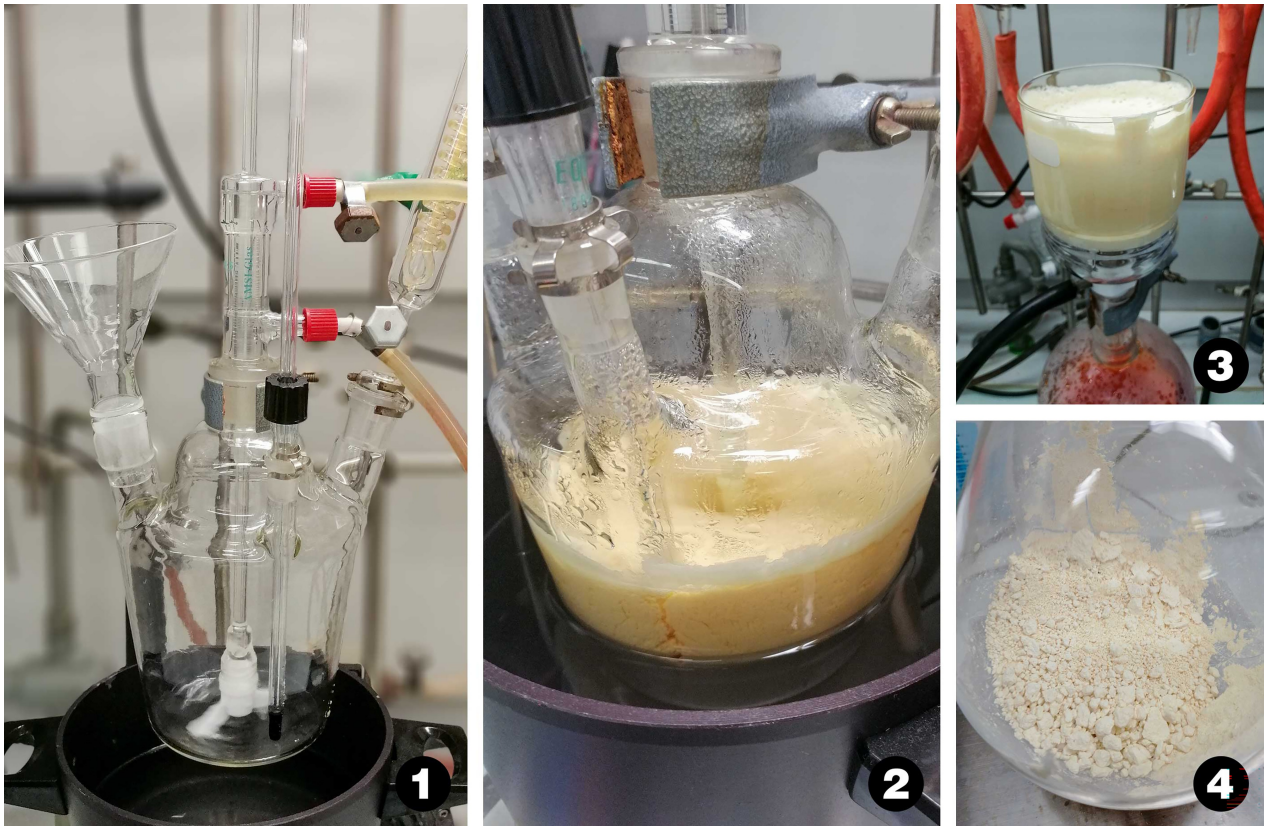

Figure 2. (1) Reaction apparatus. (2) The reaction vessel after precipitation of large amounts of yellow precipitate. (3) Filtration of and washing of the product. (4) The dried dihydrotetrazine **2**.

the dropping funnel over 5 min. An internal temperature of below 10 °C was maintained and evolution of nitrous gases (caution!) was observed as brown vapor (*Figure 3–2*). After complete addition, the valve of the dropping funnel was closed leaving the pressure equalizing tube as only outlet for the nitrous gases (*Figure 3–3*; *Note 14*). With the valve closed, the red suspension was stirred for 3.5 h while cooling with an ice water/bath leading to the formation of a bright red slurry (*Note 15*). Upon completion of the reaction, the cooling bath was removed as well as the stopper, thermometer, and dropping funnel. The reaction flask was purged for 1 min by air stream to remove most of the nitrous gases (caution!). The slurry was transferred into a separatory funnel (2 L) and CH_2Cl_2 (300 mL) and H_2O (200 mL) were added to achieve proper phase separation. The layers were separated, and the aqueous layer was extracted with CH_2Cl_2 (3×250 mL). The combined organic layers were washed once with an aqueous potassium carbonate solution (1×250 mL, 12.5 g K_2CO_3 in 250 mL H_2O), dried over anhydrous sodium sulfate (200 g), filtered through a glass funnel plugged with cotton and concentrated under reduced pressure (40 °C, 750 mbar to 30 mbar). The red solid was suspended in cold MeCN (150 mL, 4 °C) and was filtered through a glass filter frit (pore size 4). The bright red solid was dried under high vacuum to afford tetrazine **3** (33.9 g, 125 mmol, >98 % (>90 %); *Figure 3–4*; *Notes 16* and *17*).

D. **3-(3,5-Dimethyl-1*H*-pyrazol-1-yl)-6-hydrazinyl-1,2,4,5-tetrazine** (**4**)

A sulfonation flask (1.5 L, four-necked) was equipped with a mechanical overhead stirrer fitted with an uncooled stirrer bearing, two glass stoppers, and a wide necked glass funnel (NS29) under air atmosphere. Consecutively, tetrazine **3** (33.0 g, 122 mmol, 1.00 equiv.) and MeCN (300 mL) were added through the funnel resulting in a red suspension (*Figure 4–1*). The funnel was removed and while stirring (~ 300 rpm), hydrazine monohydrate (7.00 mL, 122 mmol, 1.00 equiv., 17.5M (*Note 3*)) was added continuously over 20 seconds by volumetric pipette. During addition, the suspension considerably darkened, and the starting material dissolved (*Figure 4*, 5 seconds, 10

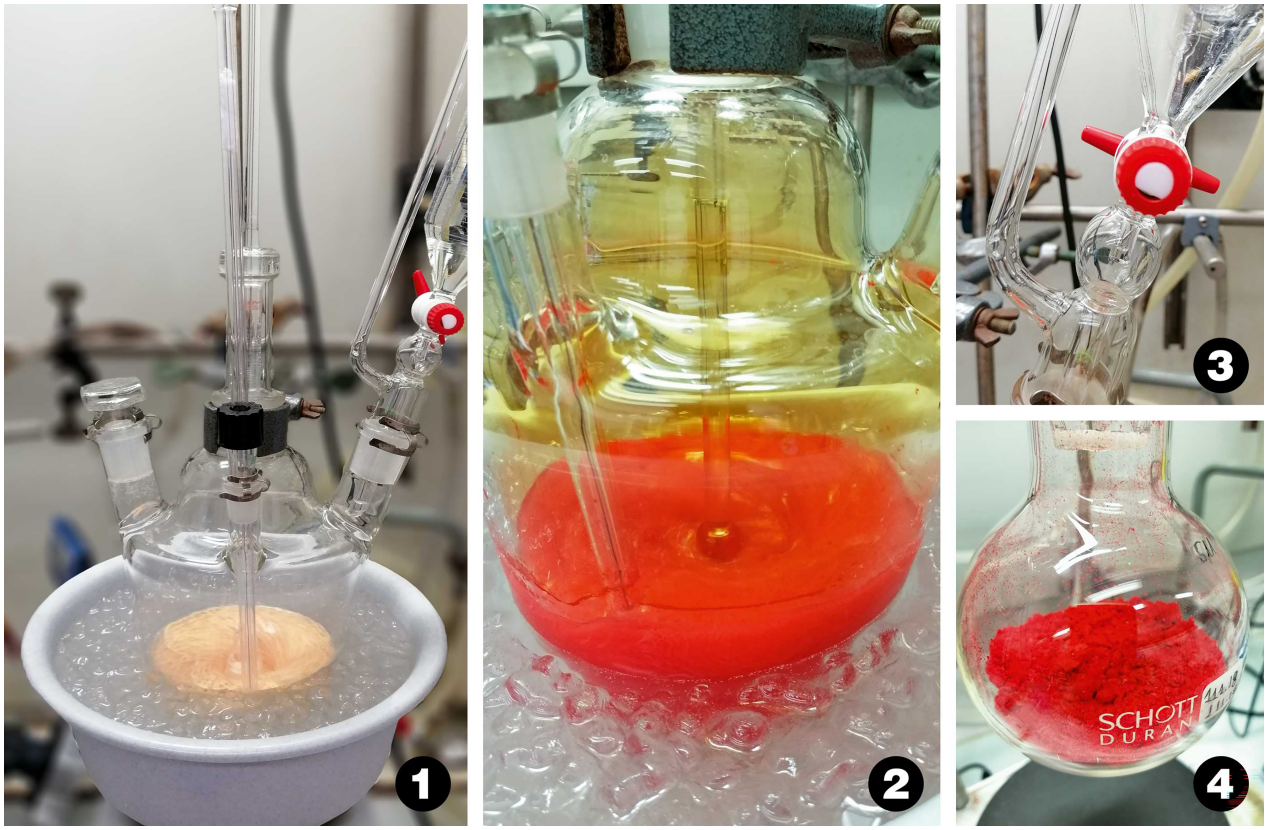

Figure 3. Reaction set-up and tetrazine **3**. (1) Reaction apparatus and reaction mixture during addition of $NaNO_2$ solution. (2) Formation of nitrous gases after addition of glacial acetic acid. (3) The closed dropping funnel valve. (4) The oxidized product **3**.

seconds, 20 seconds, 30 seconds). Within the next minute, extensive amounts of the desired product precipitated (*Figure 4*, 60 seconds; *Note 18*). The precipitate was filtered through a glass filter frit (pore size 4), and the filter cake was washed with cold toluene (2×100 mL, 4 °C; *Note 19*). The residue was dried under high vacuum to afford tetrazine **4** (17.5 g, 85.0 mmol, 70 % (68 %–78 %)) as a bright red solid (*Figure 4–2*; *Notes 20*, *21*).

E. 3-(3,5-Dimethyl-1*H*-pyrazol-1-yl)-1,2,4,5-tetrazine (**5**)

A sulfonation flask (1.5 L, four-necked) was equipped with a mechanical overhead stirrer fitted with an uncooled stirrer bearing, a glass stopper, a thermometer, and a wide necked glass funnel (NS29) under air atmosphere. Tetrazine **4** (13.3 g, 64.5 mmol, 1.00 equiv.) and THF (260 mL) were added subsequently through the funnel and the orange/red mixture was cooled to below 5 °C by an ice/water bath while stirring (260 rpm; *Figure 5–1*). Activated manganese dioxide (37.4 g, 387 mmol, 6.00 equiv.) was added in portions by spatula over 15 min during which a color change of the liquid phase of the suspension from red to purple and evolution of gas was observed (caution!). After complete addition, the suspension was stirred (~260 rpm) with continued cooling for 30 min (*Figure 5–2*; *Note 22*). Then, the mixture was filtered through a pad of *Celite*® (2 cm) and the filter cake was rinsed with CH_2Cl_2 (2× 200 mL). The filtrate was concentrated under reduced pressure (40 °C, 500 mbar to 30 mbar) resulting in a dark red solid residue. The residue was dissolved in CH_2Cl_2 (~30 mL) and purified by column chromatography (~400 g SiO_2, 30 g SiO_2 per 1.0 g of starting material, 40 cm ×5.5 cm (*h*×*d*), CH_2Cl_2 + 5 to 10 % acetone; *Note 23*; *Figure 5–3*). Removal of the solvent under reduced pressure (40 °C, 600 mbar to 200 mbar) and drying under high vacuum afforded tetrazine **5** (7.02 g, 39.9 mmol, 62 % (62 %–65 %) as a pink/red solid (*Figure 5–4*; *Notes 24*, *25*).

F. 3-Hydrazinyl-1,2,4,5-tetrazine (**6**)

A round bottom flask (1 L, one-necked (NS29)) was equipped with a 3 cm *Teflon*-coated magnetic stirring

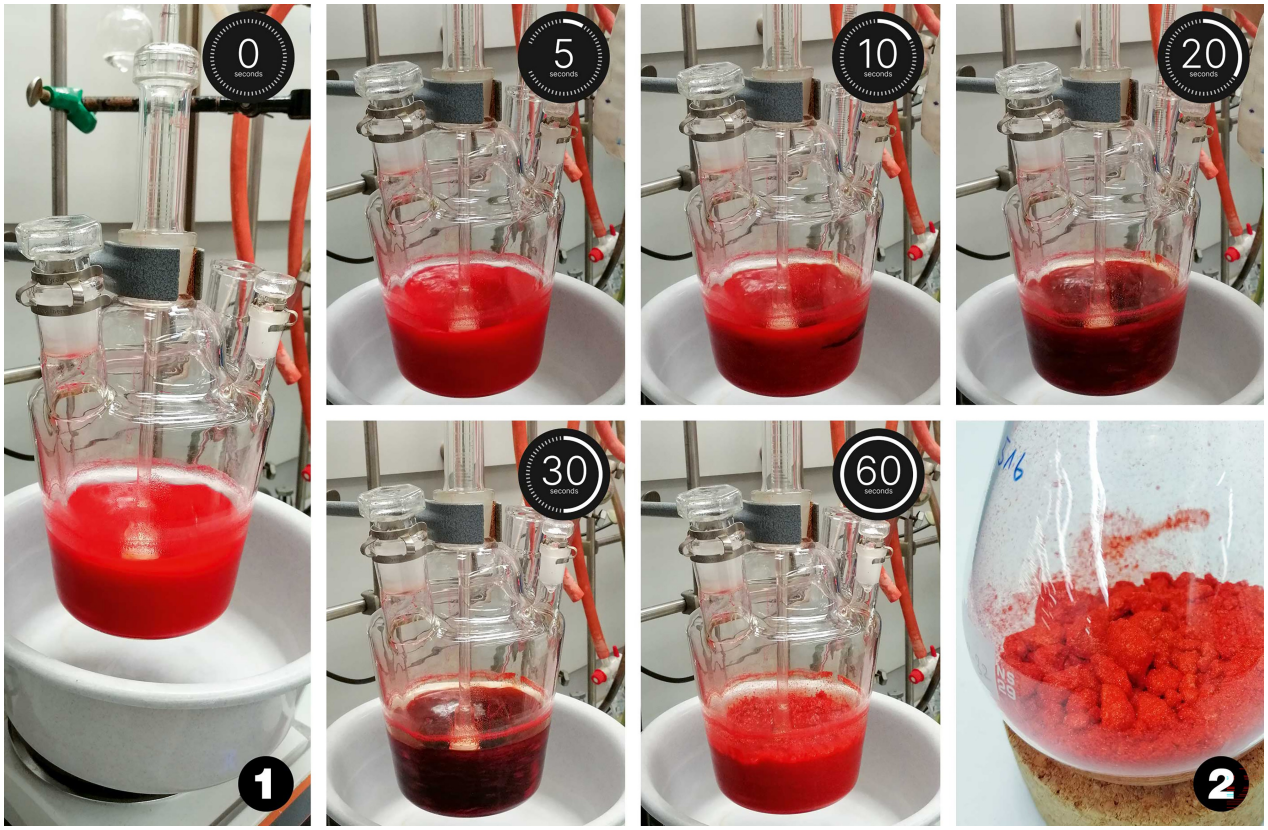

Figure 4. Progression of the reaction. (1) Reaction apparatus before addition of hydrazine. Top row: 5 seconds after addition started, 10 s after addition started, 20 s after addition started. Bottom row: 30 s after addition started, within 1 min after addition started. (2) The washed and dried asymmetric tetrazine **4**.

bar and a wide necked glass funnel (NS29) under air atmosphere. Tetrazine **5** (11.3 g, 64.1 mmol, 1.00 equiv.) and MeCN (300 mL) were added subsequently through the funnel (*Figure 6–1*). The funnel was removed and hydrazine monohydrate (3.39 mL, 57.7 mmol, 0.90 equiv., 17.5M (*Note 3*)) was added dropwise over 1 min by syringe through the open neck resulting in darkening of the mixture (*Figure 6–2*). The mixture was stirred for 15 min at room temperature followed by removal of the solvent by means of a rotary evaporator (40 °C, 300 mbar to 30 mbar) affording the crude product as brown/orange solid (*Note 26*). After the residue was washed with cold diethyl ether (3×40 mL; *Note 27*; *Figure 6–3*) and dried under high vacuum, tetrazine **6** (4.88 g, 43.5 mmol, 68% (68–82%)) was obtained as a red solid (*Figure 6–4*; *Notes 28*, *29*).

G. **3-Bromo-1,2,4,5-tetrazine** (**7**)

A round bottom flask (100 mL, one-necked (NS29)) equipped with a 2 cm *Teflon*-coated magnetic stirring bar and a septum was flame dried three times by means of a heat gun under high vacuum and subsequent flushing with N_2 and cooled to room temperature. The flask was charged with tetrazine **6** (2.00 g, 17.8 mmol, 1.00 equiv.) (*Note 30*). Subsequent addition of dry CH_2Cl_2 (36.0 mL) resulted in a red suspension (*Figure 7–1*) and the mixture was cooled by an ice/water bath while stirring. After 5 min, dibromoisocyanuric acid (DBI, 7.98 g, 26.7 mmol, 1.50 equiv.) was added in portions by spatula (*Note 30*) to the cooled suspension over 15 min while vigorously stirring (600 rpm). After complete addition, the cooling bath was removed, and the mixture was allowed to warm to room temperature (*Figure 7–2*; *Note 31*). After 1 h, the mixture was filtered through a pad of *Celite*® (2 cm) covered with SiO_2 (0.5 cm). The filter cake was rinsed with CH_2Cl_2 (3×35 mL) until the eluting filtrate became colorless. The filtrate was concentrated under reduced pressure (25 °C, 500 mbar to 350 mbar) until ~5 mL solution remained (*Figure 7–3*; *Note 32*). The mixture was purified by column chromatography (~150 g SiO_2, 20 cm ×4.5 cm, 100% CH_2Cl_2; *Figure 7–4*;

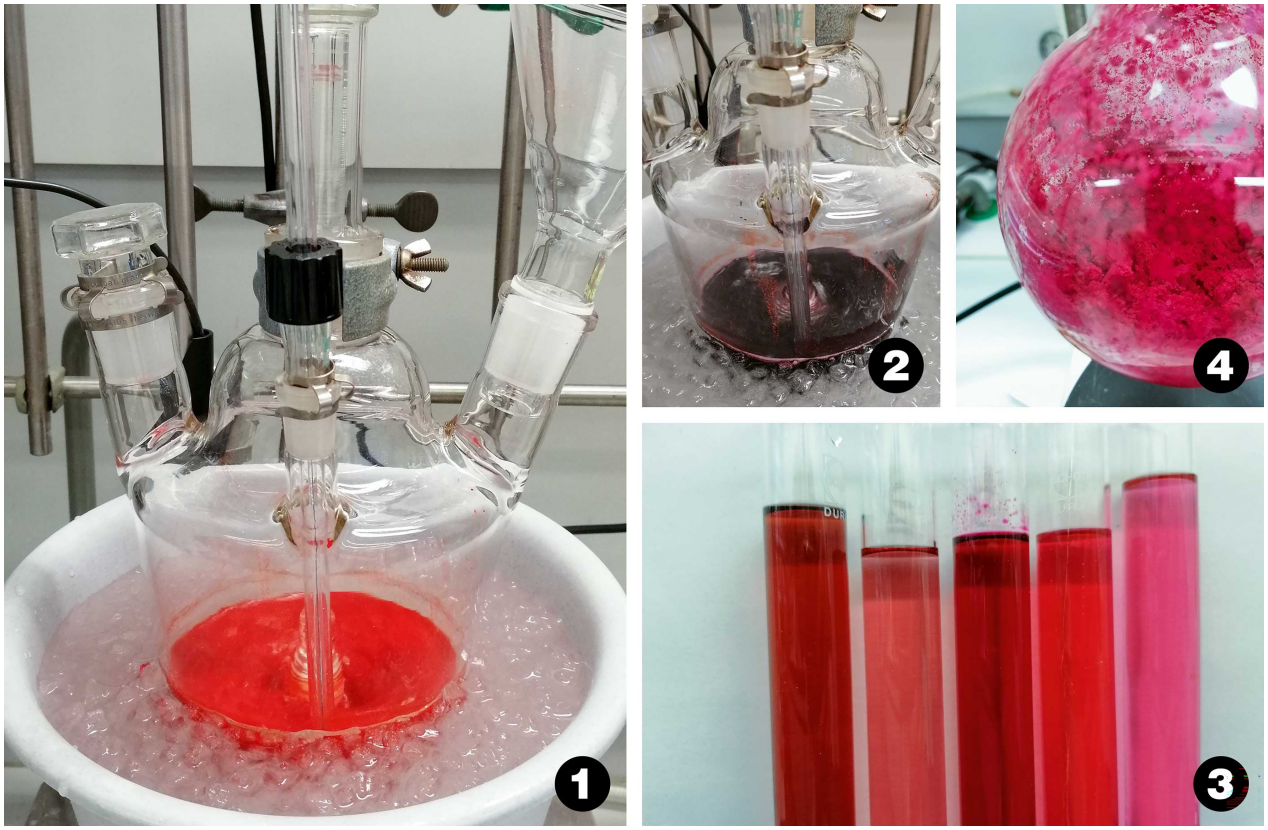

Figure 5. (1) Reaction apparatus before MnO_2 addition. (2) Reaction apparatus during MnO_2 addition and evolution of gas. (3) Possible colors of fractions during column chromatography. (4) Monosubstituted tetrazine **5**.

Note 33). Removal of the solvent under reduced pressure (25 °C, 500 mbar to 300 mbar) and drying at (25 °C, 30 mbar) for 10 min afforded 3-bromotetrazine (**7**) (2.05 g, 12.7 mmol, 72% (60–72%)) as a bright orange, crystalline solid (*Figure 7–5*) (*Notes 34*, *35*).

Discussion

Monosubstituted *s*-tetrazines have emerged over the last years as privileged building blocks for number of applications.[11] Among the different synthetic approaches to access those compounds,[11–13] 3-halogen-substituted 1,2,4,5,–tetrazines such as the title compound 3-bromo-tetrazine (**7**) offer unprecedented flexibility for late stage diversification[7,8] and a number of applications by direct reaction with target compounds. Our group demonstrated amino acid and protein labelling with subsequent click reactions,[7] enhancement of antibiotic activity by late-stage diversification,[14] or preparation of clickable tetrazine-based amino acids for solid-phase synthesis.[7] 3-Bromotetrazine **7** was shown to be susceptible to nucleophilic attack on nitrogen,[15] leading to unusual alkyl-hydro-tetrazines through an interesting mechanism,[15,16] and the products were further converted to novel heterocycles.[15] 3-Bromo pyridazines could be accessed from this building block **7**, as subsequent downstream products.[17] 3-Bromotetrazine **7** was further diversified by cross-coupling reactions,[18] and a data science-guided computational approach[19] led to the improvement of catalyst systems and broadening of substrate scope,[20] even extending into 1,2,3-triazines.[21] Many more interesting use cases have been published by other groups recently. Novel Far-Red and Near-Infrared Dyes have been enabled through the corresponding methylamine tetrazine.[22] The exceptional rate acceleration of mono-substituted tetrazine amino acids derived from the title compound **7** has been corroborated.[23] Such tetrazines could be utilized for drug release based on dynamic chemistry.[24,25] Metal complexes of monosubstituted pyridyl-tetrazines accessible from the title compound **7** were shown to feature excellent rate constants in biorthogonal chemistry.[26,27] Beyond the many biological and biomedical applications of

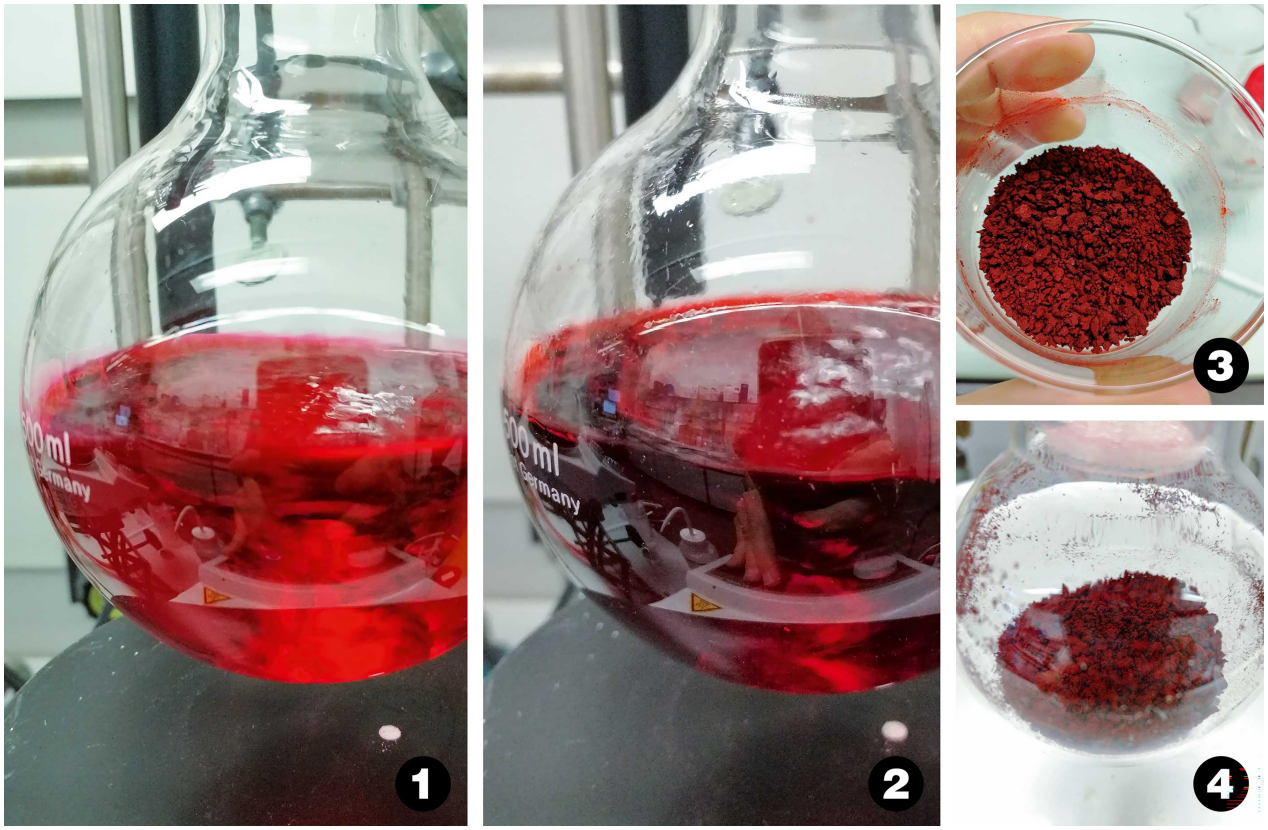

Figure 6. (1) Reaction mixture before hydrazine addition. (2) Reaction mixture after hydrazine addition. (3) The filtered and washed product. (4) The dried tetrazine **6**.

tetrazines,[28] mono substituted halogenated tetrazines have been used in high energy material applications,[29] such as tris(tetrazine)amine[30] or poly-nitro-alkoxy-tetrazines.[31] Overall, the documented and potential use of bromotetrazine **7** led to its recent commercialization (*Note 36*). For all these reasons, we anticipate that this synthetic procedure, the technical aspects, and the data it details will be useful to the practitioner in the field.

Notes

1. **Caution**: Prior to performing each reaction, a thorough hazard analysis and risk assessment should be carried out regarding each chemical substance and experimental operation on the scale planned and in the context of the laboratory where the procedures will be carried out. Proper personal protective equipment and appropriate laboratory safety measures must be installed and followed. Our group has previously assessed and published[7] the sensitivity of products and several intermediates obtained during the synthesis with regard to impact (BAM), friction (BAM), and electrostatic discharge. Furthermore, compounds **1** and **7** were subjected to differential thermal analysis. None of these analyses revealed concerning energetic behavior of the respective compounds. Nonetheless, potential high energy properties and energy liberation cannot be ruled out.
2. The following reagents, solvents and materials were purchased from commercial sources and used as received without additional purification. Guanidine hydrochloride (≥98%, *Sigma–Aldrich*), hydrazine hydrate (50–60%, *Sigma–Aldrich*), acetyl acetone (for synthesis, *Sigma–Aldrich*), sodium nitrite (≥97%, ACS reagent, *Sigma–Aldrich*), manganese(IV) oxide (90%, precipitated, activated, *Roth AG*), dibromoisocyanuric acid (≥97%, *TCI*), 1,4-dioxane (reagent grade, *Sigma–Aldrich*), dichloromethane (technical grade, *Thommen–Furler AG*), acetonitrile (MeCN) (≥99.9%, *Sigma–Aldrich*), tetrahydrofuran (≥99.9%, 250 ppm BHT, *Sigma–Aldrich*), silica gel (high-

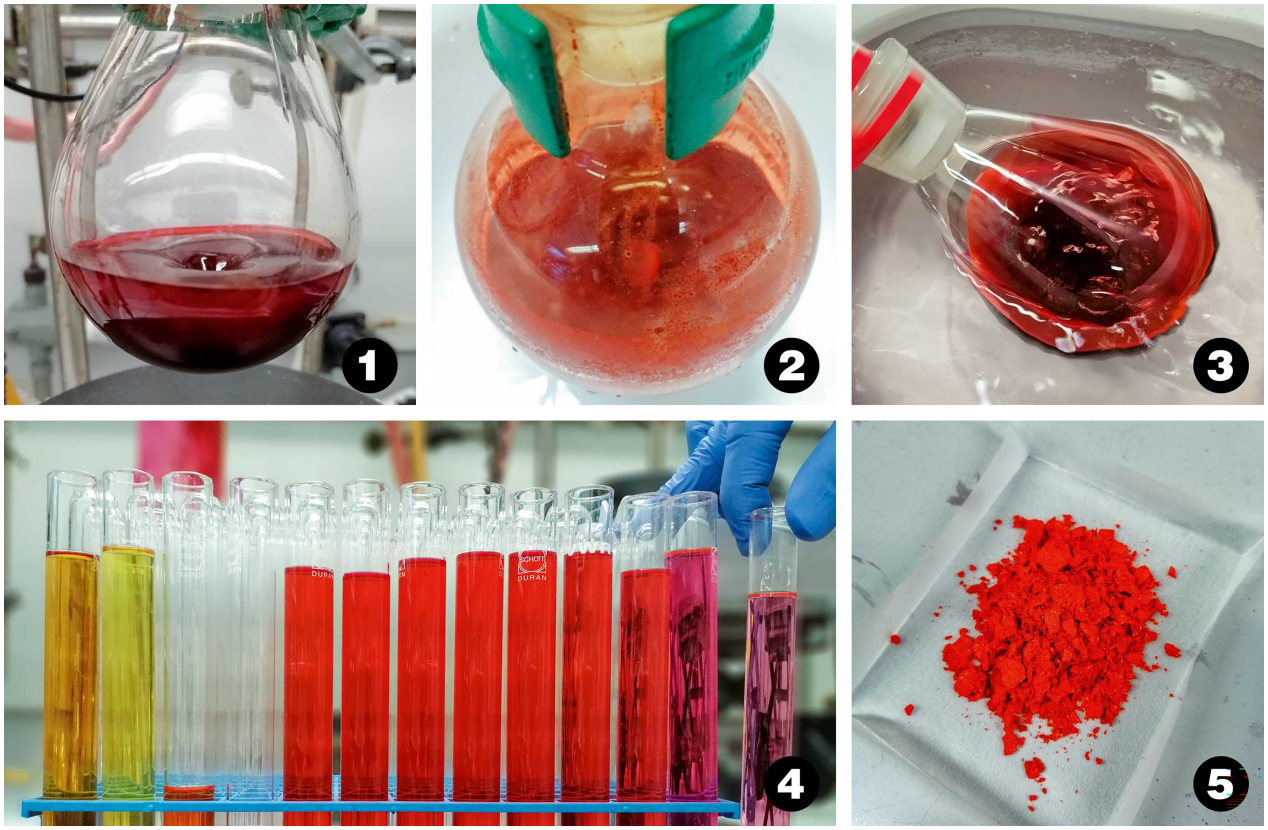

Figure 7. (1) Reaction mixture before addition of dibromoisocyanuric acid. (2) Reaction mixture after addition of dibromoisocyanuric acid. (3) Concentration of the filtrate. (4) Column chromatography fractions and their colors. (5) Bromotetrazine **7**.

purity grade (w/ Ca ~0.1%), pore size 60 Å, 230–400 mesh particle size, *Sigma–Aldrich*).

3. The hydrazine concentration was determined upon opening of a new bottle by titration against aq. HCl (100 mL, 0.1M). The equivalence point was determined by plotting the titration curve. The added amount of commercial hydrazine hydrate at the equivalence point was used to calculate the hydrazine concentration.
4. Reaction control for this reaction was not performed due to the nature of the starting material and compound **1**. A reaction time of 2 h proved to reliably provide the product with a good yield and resulted in few impurities during *step B*.
5. While drying, the yellowish solid first turned purple before becoming colorless (*Figures 1–3*, *1–4*, and *1–5*). Colors can be more or less pronounced between different experiments.
6. Characterization of the colorless crystalline solid **1**: M.p. 236.3–238.0 °C (1,4-dioxane). ^{1}H-NMR (400 MHz, D_2O): no signals observed. ^{13}C-NMR (101 MHz, D_2O): 159.5. IR (neat): 3318m, 3186s, 1668s, 1615s, 1320m, 1127m, 947s, 740w, 600s.
7. Product **1** is bench-stable over multiple weeks. However, a slow color change from colorless to pale yellow/beige can be observed.
8. The reaction was monitored by UHPLC-(+)-MS. Since the starting material was not observable, the progress of the reaction was followed by means of the intermediate with $m/z = 232$. When no more progress (decrease of the intermediate) was observed, the reaction was stopped.
9. Cold water (230 mL) was added followed by thorough mixing until a homogeneous slurry was obtained. Only then, vacuum was applied and the liquid phase removed. This procedure was repeated twice.
10. Characterization of the pale yellow solid **2**: M.p. 123.5–125.4 °C (H_2O). ^{1}H-NMR (400 MHz, $CDCl_3$): 8.10 (s, 2H), 5.98 (s, 2H), 2.49 (s, 6H), 2.23 (s, 6H). ^{13}C-NMR (101 MHz, $CDCl_3$): 150.0, 145.8, 142.3, 109.9, 13.8, 13.5. IR (neat): 3286m, 2926w, 1679m, 1614w, 1568m, 1472m, 1407s, 1371s, 1359s, 1146w, 1112w, 1060 m, 1027w, 984m, 960m, 872w, 816m, 801m, 787m, 763m, 725w, 681m, 652m, 621m, 584w, 511w, 476m. Purity was

assessed by quantitative ^{1}H-NMR (d1 = 60 sec, analyte: 26.19 mg, 1,3,5-trimethoxybenzene (≥ 99 %, *Sigma–Aldrich*): 33.67 mg) to be ≥ 93 %.

11. Upon prolonged exposure of the compound to air atmosphere slow oxidation to **3** is observed, visually accompanied by a color change to red.
12. Compound **2** can be submitted to procedure C without drying, without impact on yield or purity.
13. The following experiment was performed in a laboratory specifically equipped to work with hazardous fumes due to the evolution of nitrous gases.
14. This ensured the release of the nitrous gases from the reaction vessel at a rate slow enough for the reaction to reliably run to completion.
15. After 3 h, a sample of the mixture was taken (both phases!), the solvent removed, and a ^{1}H-NMR-spectrum was measured. If starting material (*Note 10*) was detected, another portion of $NaNO_2$ (1.50 equiv., as solid) and glacial acetic acid (1.25 equiv.) was added sequentially.
16. Characterization of the bright red solid **3**: M.p. 221.6–222.4 °C (CH_2Cl_2). ^{1}H-NMR (400 MHz, $CDCl_3$): 6.20 (s, 2H), 2.71 (s, 6H), 2.39 (s, 6H). ^{13}C-NMR (101 MHz, $CDCl_3$): 159.3, 154.4, 143.8, 111.9, 14.7, 13.8. IR (neat): 3086w, 2930w, 1729w, 1622w, 1577m, 1481s, 1422s, 1381s, 1351m, 1275m, 1162w, 1139w, 1109w, 1078 s, 1048 m, 1024 m, 967s, 942m, 845m, 794w, 757m, 659w, 623w, 588w, 563m, 543m, 511w, 469m. Purity was assessed by quantitative ^{1}H-NMR (d1 = 60 sec, analyte: 20.25 mg, 1,3,5-trimethoxybenzene (≥ 99 %, *Sigma–Aldrich*): 11.63 mg) to be ≥ 97 %.
17. Product **3** is bench-stable over multiple weeks.
18. Since the reaction is complete within such a short time, reaction control was not performed during the reaction.
19. Cold toluene (100 mL) was added followed by thorough mixing for 30 sec. Only then, vacuum was applied, and the liquid phase removed. This was repeated once. ^{1}H-NMR spectroscopy can be used to identify remaining starting material (*Note 16*) in which case an additional wash with cold toluene (100 mL) was performed.
20. Characterization of the bright red solid **4**: M.p. 147.3–147.6 °C (MeCN). ^{1}H-NMR (400 MHz, (D_6)DMSO): 9.78 (s, 1H), 6.19 (s, 1H), 4.68 (s, 2H), 2.38 (s, 3H), 2.22 (s, 3H). ^{13}C-NMR (101 MHz, (D_6)DMSO): 163.0, 157.0, 150.0, 141.3, 108.4, 13.3, 12.1. IR (neat): 3311w, 3210w, 3110w, 3024w, 1664w, 1572m, 1551w, 1481m, 1453m, 1433w, 1415m, 1406m, 1358w, 1276w, 1157w, 1131w, 1071 m, 1040w, 1022w, 978m, 953s, 851w, 828m, 800w, 779w, 692w, 662w, 622w, 595w, 573s, 547m, 488m. Purity was assessed by quantitative ^{1}H-NMR (d1 = 60 sec, analyte: 30.07 mg, 1,3,5-trimethoxybenzene (≥ 99 %, *Sigma–Aldrich*): 17.11 mg) to be ≥ 97 %.
21. Product **4** is bench-stable over multiple weeks.
22. Complete consumption of the starting material (m/z = 206) and formation of the product (m/z = 176) can be readily followed by UHPLC-(+)-MS.
23. Column chromatography (20 mL fractions) was started with CH_2Cl_2 + 5 % acetone as eluent for ~ 300 mL. The amount of acetone was increased by 1 % every 200 mL up to 10 % at which point it was not further increased. At first, the column appeared rather dark. At the front, a brown band was sometimes observed. After elution of this band, a deep red band followed. When the intensity of the color of the fractions started to decrease, TLC (CH_2Cl_2 + 10 % acetone) was used to detect the elution of a colorless but UV active impurity (R_f = 0.61; desired product: R_f = 0.79). At this point, fraction collection was stopped. The following fractions were collected: (1–3) brown, impurity; (7–25) deep red, desired product; (26–32) red/pink, mixed fractions.
24. Characterization of the pink/red solid **5**: M.p. 106.1–106.3 °C (CH_2Cl_2). ^{1}H-NMR (400 MHz, $CDCl_3$): 10.18 (s, 1H), 6.20 (s, 1H), 2.73 (s, 3H), 2.38 (s, 3H). ^{13}C-NMR (101 MHz, $CDCl_3$): 161.5, 157.1, 155.2, 144.4, 112.7, 15.2, 14.0. IR (neat): 3066w, 2927w, 1667w, 1578m, 1486s, 1436s, 1406s, 1388s, 1367m, 1288w, 1197w, 1157m, 1140m, 1098 m, 1033 m, 1015 m, 986w, 967s, 923s, 832m, 793m, 737m, 585w, 516s. Purity was assessed by quantitative ^{1}H-NMR (d1 = 60 sec, analyte: 24.83 mg, 1,3,5-trimethoxybenzene (≥ 99 %, *Sigma–Aldrich*): 18.14 mg) to be ≥ 97 %.
25. Product **5** is bench-stable over multiple weeks.
26. The reaction can easily be followed by TLC (CH_2Cl_2/MeOH 5 : 1). The starting material **5** has R_f = 0.88 and is observed as bright pink spot while the product is observed as orange spot with R_f = 0.63.
27. Cold Et_2O (50 mL) was added followed by thorough mixing for 30 sec. It is important to break up larger clumps of product. Only then, vacuum was applied, and the liquid phase removed. This was repeated twice. If after filtration, the product was not absolutely homogeneous and grains of a brighter orange solid were still present, it was washed again (50 mL). In case of insufficient

washing the ^{1}H-NMR showed following signals: ^{1}H-NMR (400 MHz, (D_6)DMSO): 11.99 (s, 1H), 5.73 (s, 1H), 2.15 (s, 3H), 2.08 (s, 3H). In this case, the product was washed again as described above.

28. Characterization of the red solid **6**: M.p. 83.6–84.5 °C (decomposition, MeCN). ^{1}H-NMR (400 MHz, (D_6)DMSO): 9.74 (s, 1H), 9.56 (s, 1H), 4.59 (s, 2H). ^{13}C-NMR (101 MHz, (D_6)DMSO): 164.3, 153.0. IR (neat): 2989m, 1556s, 1508s, 1109 s, 1047 m, 950s, 842s, 643m, 535s, 475s. Purity was assessed by quantitative ^{1}H-NMR (d1 = 60 sec, analyte: 32.93 mg, 1,3,5-trimethoxybenzene (≥ 99 %, *Sigma–Aldrich*): 12.68 mg) to be ≥ 97 %.
29. Product **6** is bench-stable over multiple weeks.
30. For this purpose, the septum was shortly removed and after the addition put back in place.
31. The reaction can be easily followed by TLC (CH_2Cl_2). The starting material **6** is observable as orange spot with $R_f = 0.03$ while the product is observed as red spot with $R_f = 0.68$.
32. Removal of the solvent at 40 °C proved to be inferior to 25 °C due to degradation and formation of brightly colored degradation products. To avoid boiling of the collected CH_2Cl_2 in the collection flask of the rotary evaporator said collection flask was externally cooled by ice/water bath.
33. Within the first 50 mL of eluent, a yellow band started to separate from the front of the colored mixture. When this yellow fraction started to elute from the column, fractions (20 mL tubes) were collected. When the next orange fraction started to elute from the column smaller fractions (5 mL) were collected for two to three fractions before increasing the collected volume again (20 mL). When the collected fractions were pink instead of bright orange/red, the collection was stopped. The desired product was obtained from fractions 5–12. Suitable TLC conditions to follow the chromatography are described in *Note 31*.
34. Characterization of the bright orange crystalline solid **7**: M.p. 70.0–72.0 °C (CH_2Cl_2). ^{1}H-NMR (400 MHz, $CDCl_3$): 10.34 (s, 1H). ^{13}C-NMR (101 MHz, $CDCl_3$): 164.2, 158.0. IR (neat): 3082w, 1711w, 1485w, 1389m, 1370w, 1226m, 1204s, 1167m, 1127w, 884s. Purity was assessed by quantitative ^{1}H-NMR (d1 = 60 sec, analyte: 21.85 mg, 1,3,5-trimethoxybenzene (≥ 99 %, *Sigma–Aldrich*): 21.40 mg) to be ≥ 97 %.
35. Tetrazine **7** should be stored at −20 °C. In case of frequent use and therefore warming to room temperature, aliquotation of reasonable amounts is advised. After repeated warming from −20 to 25 °C, slow degradation to an unknown product is observed. This impurity can be removed by dissolving **7** in CH_2Cl_2 and removal of the insoluble parts by filtration through a glass filter frit (pore size 4). Upon concentration *in vacuo* (25 °C, 400 to 10 mbar) pure compound **7** is again obtained.
36. The authors of the present synthetic procedure have not been and are currently not involved in the selling, marketing, commercialization, distribution, *etc.* of the title compound and do not have any financial interest.

Acknowledgements

Open Access funding provided by Universität Zürich.

Author Contribution Statement

L. V. H., *S. D. S.*, and *K. G.* conceived and designed the study and the experiments. *L. V. H.*, *S. D. S.*, *E. B.*, *F. P. F.*, *A. T.* carried out the experiments, *K. G.* organized funding. *K. G.* and *M. R.* supervised the study, *L. V. H.* and *M. R.* contributed to the visual design, *L. V. H.* and *K. G.* wrote the paper with input from all authors. All authors approved the final version of the manuscript.

References

[1] A. Pinner, 'Ueber die Einwirkung von Hydrazin auf Imidoäther', *Ber. Dtsch. Chem. Ges.* **1893**, *26*, 2126–2135.
[2] Z. Li, J. Ding, N. Song, X. Du, J. Zhou, J. Lu, Y. Tao, 'Alternating Copolymers of Dithienyl-s-Tetrazine and Cyclopentadithiophene for Organic Photovoltaic Applications', *Chem. Mater.* **2011**, *23*, 1977–1984.
[3] D. K. Hwang, R. R. Dasari, M. Fenoll, V. Alain-Rizzo, A. Dindar, J. W. Shim, N. Deb, C. Fuentes-Hernandez, S. Barlow, D. G. Bucknall, P. Audebert, S. R. Marder, B. Kippelen, 'Stable Solution-Processed Molecular *n*-Channel Organic Field-Effect Transistors', *Adv. Mater.* **2012**, *24*, 4445–4450.
[4] M. L. Landry, G. M. McKenna, N. Z. Burns, 'Enantioselective Synthesis of Azamerone', *J. Am. Chem. Soc.* **2019**, *141*, 2867–2871.
[5] D. L. Boger, J. Hong, 'Asymmetric Total Synthesis of *ent*-(−)-Roseophilin: Assignment of Absolute Configuration', *J. Am. Chem. Soc.* **2001**, *123*, 8515–8519.
[6] W. Kaim, 'The coordination chemistry of 1,2,4,5-tetrazines', *Coord. Chem. Rev.* **2002**, *230*, 127–139.
[7] S. D. Schnell, L. V. Hoff, A. Panchagnula, M. H. H. Wurzenberger, T. M. Klapötke, S. Sieber, A. Linden, K. Gademann, '3-Bromotetrazine: labelling of macromolecules *via* mono-

substituted bifunctional *s*-tetrazines', *Chem. Sci.* **2020**, *11*, 3042–3047.

[8] E. Ros, M. Bellido, X. Verdaguer, L. Ribas de Pouplana, A. Riera, 'Synthesis and Application of 3-Bromo-1,2,4,5-Tetrazine for Protein Labeling to Trigger Click-to-Release Biorthogonal Reactions', *Bioconjugate Chem.* **2020**, *31*, 933–938.

[9] J. Zhu, J. Hiltz, R. B. Lennox, R. Schirrmacher, 'Chemical modification of single walled carbon nanotubes with tetrazine-tethered gold nanoparticles *via* a Diels–Alder reaction', *Chem. Commun.* **2013**, *49*, 10275–10277.

[10] D. E. Chavez, M. A. Hiskey, 'Synthesis of the bi-heterocyclic parent ring system 1,2,4-triazolo[4,3-*b*][1,2,4,5]tetrazine and some 3,6-disubstituted derivatives', *J. Heterocycl. Chem.* **1998**, *35*, 1329–1332.

[11] J. Mondal, A. Sivaramakrishna, 'Functionalized Triazines and Tetrazines: Synthesis and Applications.', *Top. Curr. Chem.* **2022**, *380*, 34.

[12] Y. Qu, F.-X. Sauvage, G. Clavier, F. Miomandre, P. Audebert, 'Metal-Free Synthetic Approach to 3-Monosubstituted Unsymmetrical 1,2,4,5-Tetrazines Useful for Bioorthogonal Reactions', *Angew. Chem. Int. Ed.* **2018**, *57*, 12057–12061.

[13] Y. Xie, Y. Fang, Z. Huang, A. M. Tallon, C. W. am Ende, J. M. Fox, 'Divergent Synthesis of Monosubstituted and Unsymmetrical 3,6-Disubstituted Tetrazines from Carboxylic Ester Precursors', *Angew. Chem. Int. Ed.* **2020**, *59*, 16967–16973.

[14] A. Dorst, R. Berg, C. G. W. Gertzen, D. Schäfle, K. Zerbe, M. Gwerder, S. D. Schnell, P. Sander, H. Gohlke, K. Gademann, 'Semisynthetic Analogs of the Antibiotic Fidaxomicin–Design, Synthesis, and Biological Evaluation', *ACS Med. Chem. Lett.* **2020**, *11*, 2414–2420.

[15] S. D. Schnell, M. Schilling, J. Sklyaruk, A. Linden, S. Luber, K. Gademann, 'Nucleophilic Attack on Nitrogen in Tetrazines by Silyl-Enol Ethers', *Org. Lett.* **2021**, *23*, 2426–2430.

[16] R. Ketkaew, F. Creazzo, S. Luber, 'Closer Look at Inverse Electron Demand Diels–Alder and Nucleophilic Addition Reactions on *s*-Tetrazines Using Enhanced Sampling Methods', *Top. Catal.* **2022**, *65*, 1–17.

[17] S. D. Schnell, J. A. González, J. Sklyaruk, A. Linden, K. Gademann, 'Boron Trifluoride-Mediated Cycloaddition of 3-Bromotetrazine and Silyl Enol Ethers: Synthesis of 3-Bromo-pyridazines', *J. Org. Chem.* **2021**, *86*, 12008–12023.

[18] L. V. Hoff, S. D. Schnell, A. Tomio, A. Linden, K. Gademann, 'Cross-Coupling Reactions of Monosubstituted Tetrazines', *Org. Lett.* **2021**, *23*, 5689–5692.

[19] L. Hoff, G. A. Chesnokov, A. Linden, K. Gademann, 'DFT Featurization of 730 Commercially Available Boronic Acids (1.0.0) [Data set]', 2023, DOI 10.5281/zenodo.7540235.

[20] L. V. Hoff, G. A. Chesnokov, A. Linden, K. Gademann, 'Mechanistic Studies and Data Science-Guided Exploration of Bromotetrazine Cross-Coupling', *ACS Catal.* **2022**, *12*, 9226–9237.

[21] L. V. Hoff, J. M. Hauser, K. Gademann, 'Cross-Coupling Reactions of 5-Bromo-1,2,3-triazine', *J. Org. Chem.* **2022**, *87*, 15684–15692.

[22] W. Mao, W. Chi, X. He, C. Wang, X. Wang, H. Yang, X. Liu, H. Wu, 'Overcoming Spectral Dependence: A General Strategy for Developing Far-Red and Near-Infrared Ultra-Fluorogenic Tetrazine Bioorthogonal Probes', *Angew. Chem. Int. Ed.* **2022**, *61*, e202117386.

[23] E. Ros, M. Bellido, J. A. Matarin, A. Gallen, M. Martínez, L. Rodríguez, X. Verdaguer, L. Ribas de Pouplana, A. Riera, 'Amino acids with fluorescent tetrazine ethers as bioorthogonal handles for peptide modification', *RSC Adv.* **2022**, *12*, 14321–14327.

[24] M. D. Perretti, Y. Pérez-Pérez, K. Soler-Carracedo, E. Martín-Encinas, C. Alonso, J. Scoccia, R. Carrillo, 'Hydrogen sulphide-triggered theranostic prodrugs based on the dynamic chemistry of tetrazines', *Chem. Commun.* **2022**, *58*, 5518–5521.

[25] T. Santos, D. S. Rivero, Y. Pérez-Pérez, E. Martín-Encinas, J. Pasán, A. H. Daranas, R. Carrillo, 'Dynamic Nucleophilic Aromatic Substitution of Tetrazines', *Angew. Chem. Int. Ed.* **2021**, *60*, 18783–18791.

[26] M. Schnierle, S. Blickle, V. Filippou, M. R. Ringenberg, 'Tetrazine metallation boosts rate and regioselectivity of inverse electron demand Diels–Alder (iEDDA) addition of dienophiles', *Chem. Commun.* **2020**, *56*, 12033–12036.

[27] M. Schnierle, M. Winkler, V. Filippou, J. van Slageren, M. R. Ringenberg, '(Spectro)Electrochemistry of 3-(Pyrid-2-yl)-*s*-Tetrazine- and 1,2-(Dihydro)pyridazine Tricarbonylrhenium(I)chloride', *Eur. J. Inorg. Chem.* **2022**, e202100998.

[28] H. Sun, Q. Xue, C. Zhang, H. Wu, P. Feng, 'Derivatization based on tetrazine scaffolds: Synthesis of tetrazine derivatives and their biomedical applications', *Org. Chem. Front.* **2022**, *9*, 481–498.

[29] L. L. Fershtat, 'Recent advances in the synthesis and performance of 1,2,4,5-tetrazine-based energetic materials', *FirePhysChem* **2023**, *3*, 78–87.

[30] G. F. Rudakov, Y. A. Moiseenko, N. A. Spesivtseva, 'Synthesis of monosubstituted 1,2,4,5-tetrazines – 3-amino-1,2,4,5-tetrazines', *Chem. Heterocycl. Compd.* **2017**, *53*, 802–810 (in Russian).

[31] G. F. Rudakov, A. I. Kalinichenko, T. Q. Nguyen, S. S. Zinchenko, G. V. Cherkaev, I. V. Fedyanin, V. P. Sinditskii, 'Monosubstituted Polynitroalkoxy-1,2,4,5-Tetrazines: A New Family of Melt-Castable Energetic Materials', *Propellants Explos. Pyrotech.* **2022**, *47*, e202100262.

Received December 22, 2022
Accepted January 31, 2023

